Fabrication of epitaxial CrO_2 nanostructures directly on MgO(100) by pulsed laser deposition

N. F. Heinig, H. Jalili, and K. T. Leung[a)]
Departments of Chemistry and Physics, University of Waterloo, Waterloo, Ontario N2L 3G1, Canada

(Received 26 June 2007; accepted 15 November 2007; published online 17 December 2007)

Single-phase CrO_2 nanostructured thin films have been grown directly on MgO(100) by pulsed laser ablation of a metallic Cr target in an O_2 environment. X-ray diffraction shows that these films are strained and consist of CrO_2 crystallites with two possible epitaxial relationships to the substrate; either $CrO_2(110)$ or $CrO_2(200)$ is parallel to MgO(100). Scanning electron microscopy and atomic force microscopy reveal orthogonally arranged nanoneedles and platelike structures (both 30–50 nm thick). X-ray photoemission confirms that the films are primarily CrO_2 covered with a thin CrO_3 overlayer and indicates its complete synthesis without any residual metallic Cr. © *2007 American Institute of Physics*. [DOI: 10.1063/1.2822394]

Chromium dioxide is known to be the only ferromagnetic, metallic, binary oxide[1] and it has long been a technologically important material, widely used as a particulate recording medium for magnetic tapes. CrO_2 could also be a useful material in the emerging field of spin-transport electronics.[2] In 1986, Schwarz[3] predicted that CrO_2 was half metallic from density-of-states calculations. A year later, this was partially confirmed by Kämper *et al.*,[4] who observed nearly 100% spin polarization within 2 eV below the Fermi edge by spin-polarized photoemission. Half-metallic materials are generally characterized by one spin orientation exhibiting a metallic band structure, while the other orientation has a semiconductorlike gap at the Fermi edge. This large carrier spin polarization could make CrO_2 very useful for spin valves and spin-dependent tunnel junction devices.[1,5]

CrO_2 is metastable under ambient conditions, and special fabrication methods are needed. To date, high-quality single crystal CrO_2 films can only be grown on highly lattice-matched substrates and by using specialized growth techniques such as high-pressure synthesis[6,7] or atmospheric pressure chemical vapor deposition (CVD).[5,8] For many proposed spintronic devices, multilayer epitaxial films with high quality interfaces are necessary in order to preserve and extract the spin polarization information. Physical vapor deposition (PVD) techniques, such as molecular beam epitaxy (MBE) or pulsed laser deposition (PLD), are commonly used to fabricate multilayer films *in situ* and to develop high-quality interfaces in other material systems. Several groups have, therefore, attempted to prepare CrO_2 films on $TiO_2(100)$, Si(100), Si(111), $LaAlO_3(100)$, and $Al_2O_3(0001)$ by using MBE (Ref. 9) and PLD.[10,11] Since the most stable chromium oxide phase is Cr_2O_3, these groups have focused on reaching higher oxidation states by either reacting Cr metallic vapor with atomic oxygen in MBE (Ref. 9) or by using oxygen-rich chromium oxide targets (CrO_3 and Cr_8O_{21}) in PLD.[11] Thus far, these efforts have led to films that either exhibit weak and broad x-ray diffraction (XRD) features or contain a mixture of various chromium oxide phases, including Cr_2O_3, CrO_2, and CrO_3.

In addition to the presence of a sufficient oxygen pressure during growth, the other key parameter for producing high quality CrO_2 films is a compatible substrate that provides a good lattice match. Almost all the high quality CrO_2 films produced by either high pressure synthesis or CVD were grown on a single-crystal TiO_2 surface.[5–8] Although epitaxial growth of CrO_2 on MgO(100) has been reported, this group used a TiO_2 buffer layer prior to the growth.[12]

In the present work, we report the growth of a CrO_2 film by pulsed laser deposition using a metallic Cr target in an O_2 environment. These films were grown directly onto MgO(100) without any buffer layers. Exceptionally high laser fluences were used in order to increase the reactivity of the ablated Cr metal and, together with a high O_2 pressure, a high Cr oxidation state can be achieved. No metallic Cr was detected in the films by either x-ray photoelectron spectroscopy (XPS) or XRD, indicating complete oxidation reaction of Cr in the formation of these single-phase CrO_2 films.

A NanoPLD system (PVD Products) with a base pressure better than 5×10^{-7} Torr was used for the film growth experiments. The system was equipped with a KrF excimer laser (Lambda Physik COMpex 205). The MgO(100) substrates (99.95% purity, MTI), 5×10 mm^2 (or 10×10 mm^2) in size, were mounted on the substrate holder with silver epoxy. Metallic Cr (99.95% purity) was used as the target, with a target-to-substrate distance set to 42 mm. The pressure of O_2 (99.99% purity, Praxair) was kept constant between 10 and 900 mTorr during growth and the substrate temperature during growth could be fixed between 300 and 780 °C as monitored by a thermocouple. The films were grown for 20 min, with the laser running at a 10 Hz repetition rate and its fluence typically set at 350–550 mJ/pulse.

For each growth condition, the morphology of the resulting film was characterized by field-emission scanning electron microscopy (SEM) (LEO 1530) and atomic force microscopy (AFM) (DI Nanoscope IV) operated in tapping mode. The structure of the film was analyzed by using high-resolution XRD (PANalytical X'Pert Pro MRD) equipped with a two-bounce hybrid monochromator and a Cu K_α source. The chemical-state composition of the film was studied by using XPS (VG Scientific ESCALab 250) equipped with a monochromatic Al K_α x-ray source (1486.6 eV) at a typical energy resolution of 0.4–0.5 eV full width at half maximum. The collected XPS data were fitted with a combination of Gaussian-Lorentzian lineshapes after correction

[a)]Electronic mail: tong@uwaterloo.ca

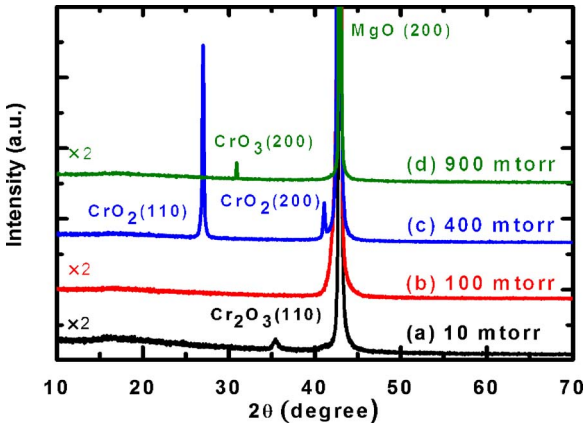

FIG. 1. (Color online) $2\theta-\omega$ XRD spectra for the CrO_x films grown on MgO(100) substrates at O_2 pressure of (a) 10 mTorr, (b) 100 mTorr, (c) 400 mTorr, and (d) 900 mTorr. The intense feature at $2\theta=42.9°$ corresponds to the MgO(200) substrate peak.

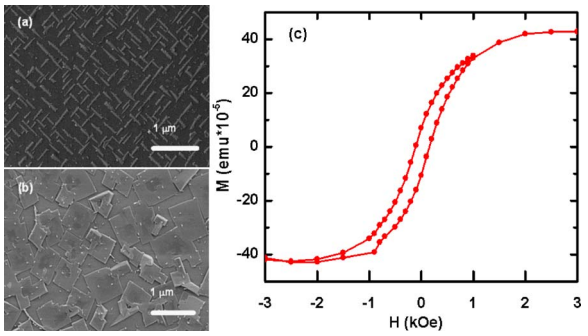

FIG. 2. (Color online) SEM images of a CrO_2 film grown at 480 °C with 400 mTorr O_2 pressure, depicting both (a) nanoneedles near the edges and corners of the sample, and (b) plates near the film center. (c) shows the magnetization (M) vs field (H) curve at 5 K, with H parallel to the film surface. The paramagnetic contribution has been subtracted from the curve.

with the Shirley background. The magnetic behavior of some films was also investigated by superconducting quantum interference device (SQUID) magnetometry (Quantum Design) at 5 K, and in fields up to 5 kOe.

Since the earlier PLD studies on chromium oxide film growth suggest that a higher oxygen pressure is necessary for CrO_2 growth,[10,11] we performed the initial PLD growth on MgO(100) with a relatively high O_2 pressure of 400 mTorr but at several substrate temperatures including 300, 400, and 480 °C. Only the samples grown at 480 °C exhibit XRD features that could be attributed to CrO_2, while the other two samples show no XRD peaks. With the substrate temperature held at 480 °C, we repeated the growth at different O_2 pressures, including 10, 100, and 900 mTorr, and the XRD data of the resulting films are shown in Fig. 1. The samples grown at 10 and 100 mTorr both appear yellow-green in color, while the samples obtained at 400 and 900 mTorr are gray and semitransparent, respectively.

The film grown at 10 mTorr exhibits a small peak at $2\theta=35.5°$ that can be attributed to $Cr_2O_3(110)$ (Ref. 13) [Fig. 1(a)]. The yellow-green color of the film is also typical of Cr_2O_3. No XRD peak was observed for the other yellow-green film grown at 100 mTorr [Fig. 1(b)], which suggests that these two films are mainly amorphous Cr_2O_3. For the semitransparent film grown at 900 mTorr, the very weak peak observed at $2\theta=31.1°$ can be assigned to $CrO_3(200)$.[14]

For the gray sample grown at 400 mTorr, there are two strong XRD peaks that could be attributed to the film [Fig. 1(c)]. We assign the peaks at $2\theta=27.1°$ and $2\theta=41.2°$ to $CrO_2(110)$ and $CrO_2(200)$, respectively, according to the powder XRD pattern,[15] which, however, shows that the $CrO_2(110)$ peak is the most intense while the $CrO_2(200)$ feature has a relative intensity of only 8%. These data suggest that the as-grown film consists of CrO_2 crystallites with two possible epitaxial relationships with the MgO(100) surface: $CrO_2(110)\|MgO(100)$and $CrO_2(200)\|MgO(100)$. The $CrO_2(200)$ peak is slightly shifted from the powder value, consistent with a 0.7% compression of the lattice. Furthermore, the $CrO_2(110)$ peak is found to be shifted from the powder value reported in the literature, consistent with a 4.8% expansion of the lattice of the as-grown film. In contrast to the bulk lattice constants of $a=b=4.421$ Å and $c=2.916$ Å, the strained CrO_2 constants can be calculated to be $a=b=4.643$ Å and $c=2.642$ Å. By using this strained unit cell, we find the off-axis peaks attributable to $CrO_2(101)$ (not shown), thus confirming the presence of CrO_2.

Of the large number of possible chromium oxides, few have diffraction peaks near the positions that we observe for the film grown at 400 mTorr [Fig. 1(c)]. The closest alternative assignment for the peak at $2\theta=27.1°$ would be $Cr_2O_5(\bar{2}21)$.[16] However, the corresponding Cr $2p$ XPS envelope is found to consist of a single peak [Fig. 3(a)], in marked contrast to the Cr_2O_5 envelope reported in the literature.[17] The observed differences in our XPS result can therefore be used to rule out the formation of Cr_2O_5.

The corresponding SEM images for the CrO_2 film grown on MgO(100) at 400 mTorr [Fig. 1(c)] are shown in Fig. 2. Needlelike nanostructures [Fig. 2(a)] with an average size of 300 nm(wide) $\times$ 1–2 μm(long) and 30–40 nm in height are found mostly near the edges and corners of the sample. These needles are distributed in an orthogonal cross pattern, suggesting an epitaxial relationship with the MgO(100) substrate. In the rest of the sample, platelike structures with an average edge size of 0.6–1.2 μm and height of 30–50 nm are seen in Fig. 2(b). The heights of these nanostructures are obtained from AFM measurements (not shown). While these morphological features are highly reproducible in the films grown at 480 °C and 400 mTorr O_2 pressure on the MgO(100) substrate, they were not observed on films grown under similar conditions on other substrates, including $LaAlO_3(100)$, $Al_2O_3(100)$, $SrTiO_3(100)$, and Si(100).[18]

Figure 2(c) shows the magnetization-field $M(H)$ curve collected at 5 K over a magnetic field range of ±5 kOe for the CrO_2 film grown at 400 mTorr. Despite the small amount of film material (estimated to be less than 3×10^{-6} cm^3), there is a clear ferromagnetic signature in the hysteretic behavior, with a coercive field of 40–60 Oe. The $M(H)$ curve for a MgO substrate was also measured at 5 K and found to be reversibly paramagnetic with no ferromagnetic impurities.

Figure 3 shows the Cr $2p$ and O $1s$ XPS spectra for the center region of the CrO_2 film grown on MgO(100) at 480 °C with 400 mTorr O_2 pressure and as a function of sputtering depth. For the as-grown film, the Cr $2p_{3/2}$ ($2p_{1/2}$) envelope [Fig. 3(a)] can be fitted to two components at 576.6 (586.4) eV and 579.3 (588.5) eV corresponding to CrO_2 and CrO_3, respectively.[19,20] The binding energy location of Cr $2p_{3/2}$ for the Cr(IV) state observed in the present work is in general accord with the earlier results.[21,22] In particular,

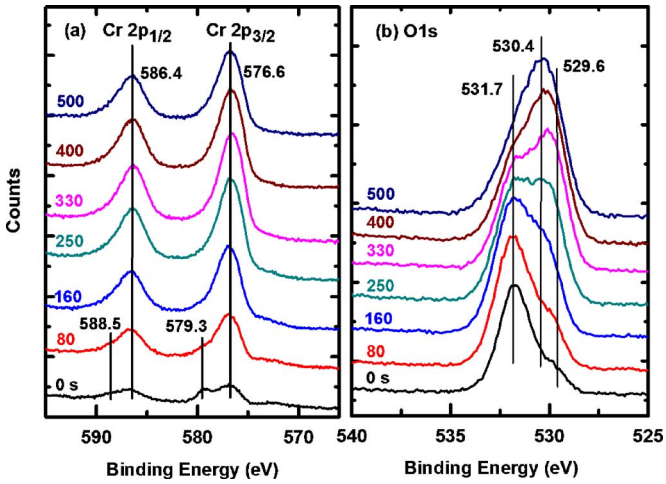

FIG. 3. (Color online) XPS spectra of (a) Cr $2p$ and (b) O $1s$ regions of a CrO_2 film as grown on MgO(100) at 480 °C with 400 mTorr O_2 pressure and upon sputtering for 80, 160, 250, 330, 400, and 500 s.

Bullen and Garrett[19] observed the CrO_2 $2p_{3/2}$ feature at 576.4 eV for the CrO_2 powder and that at 576.6 eV for a 850 nm thick CrO_2 film grown on TiO_2 by CVD. Brand *et al.*[23] reported a Cr $2p_{3/2}$ feature at 577 eV for their 21 nm thick CrO_2 film also grown on TiO_2 by CVD. Furthermore, Liu *et al.*[20] found the Cr $2p_{3/2}$ peak for bulk CrO_3 located at 579.2 eV, which is in good agreement with the weaker feature in the present work. The presence of CrO_3 is expected due to the conversion of CrO_2 to CrO_3 under a high O_2 pressure in the chamber. Upon sputtering to 160 s, the Cr $2p_{3/2}$ ($2p_{1/2}$) feature at 579.3 (588.5) eV for CrO_3 is diminished while the corresponding CrO_2 feature at 576.6 (586.4) eV strengthens. Further sputtering completely removes the CrO_3 peak, leaving behind only an intense CrO_2 feature. The observed spectral evolution upon sputtering therefore suggests that the film consists primarily of CrO_2, covered by a thin CrO_3 overlayer. The Cr $2p$ intensities of the CrO_2 features appear to reach a maximum after 330 s sputtering and then decrease upon further sputtering, consistent with a relatively thin film (<50 nm) as illustrated by the AFM images (not shown). It should be noted that despite using Cr metal as our target for growing the present film, no Cr $2p_{3/2}$ features for metallic Cr located at 574.2 eV (Ref. 24) are detected, even after sputtering for 500 s. Because the sputtered chromium feature can be fitted to a single peak, it is unlikely that the film contains other chromium oxide phases than CrO_2.

For the as-grown film, the corresponding O $1s$ envelope [Fig. 3(b)] can be fitted to three features. The intense peak at 531.7 eV can be attributed to $Mg(OH)_2$, while the two weaker features at 530.4 and 529.6 eV can be assigned to MgO and CrO_2, respectively. The observed $Mg(OH)_2$ and MgO features are evidently in good accord with the literature values (531.5 and 530.4 eV, respectively).[25] The binding energy for the observed O $1s$ feature for CrO_2 is similar to that (529.3 eV) reported by Bullen and Garrett.[19] Because the as-grown film is not continuous over the entire substrate, it is not surprising to see the large contribution from the MgO substrate and its associated surface hydroxide. The presence of the O $1s$ feature for CrO_3 (at 531 eV) (Ref. 26) is obscured by the strong substrate MgO features. Sputtering the sample for 330 s diminishes the $Mg(OH)_2$ feature, revealing the stronger MgO feature that becomes the prominent peak after further sputtering for 500 s.

Using pulsed laser ablation, we have grown CrO_2 films directly on MgO(100) substrates with a metallic Cr target in an O_2 environment. In a limited set of growth conditions (550 mJ/pulse laser fluence, 480 °C substrate temperature and 400 mTorr O_2 pressure), we are able to reproducibly grow thin, noncontinuous single phase CrO_2 films (~50 nm thick), as shown by our XRD and XPS data. The CrO_2 films consist of needle and platelike structures and are highly strained. Their ferromagnetic character is confirmed by SQUID magnetometry. The XPS results rule out the presence of metallic chromium or another amorphous chromium oxide phase. Growth of the CrO_2 phase is possible likely because of the high laser fluence and high oxygen pressures used. With further optimization, it should be possible to use the PLD method to produce high quality single crystal CrO_2 films as part of the multilayer structure appropriate for spintronic applications.

This work was supported by the Natural Sciences and Engineering Research Council of Canada. We are grateful to Dr. P. Dubé (McMaster University) and Dr. F. Razavi (Brock University) for their assistance with the magnetization measurements.

[1] J. M. Coey and M. Venkatesan, J. Appl. Phys. **91**, 10 (2002).
[2] S. A. Wolf, D. D. Awschalom, R. A. Buhrman, J. M. Daughton, S. von Molnár, M. L. Roukes, A. Y. Chtchelkanova, and D. M. Treger, Science **294**, 1488 (2001).
[3] K. Schwarz, J. Phys. F: Met. Phys. **16**, L211 (1986).
[4] K. P. Kämper, W. Schmitt, G. Güntherodt, R. J. Gambino, and R. Ruf, Phys. Rev. Lett. **59**, 2788 (1987).
[5] X. W. Li, A. Gupta, and G. Xiao, Appl. Phys. Lett. **75**, 713 (1999).
[6] R. C. DeVries, Mater. Res. Bull. **1**, 83 (1966).
[7] L. Ranno, A. Barry, and J. M. D. Coey, J. Appl. Phys. **81**, 5774 (1997).
[8] S. Ishibashi, T. Namikawa, and M. Satou, Mater. Res. Bull. **14**, 51 (1979).
[9] N. J. C. Ingle, R. H. Hammond, and M. R. Beasley, J. Appl. Phys. **89**, 4631 (2001).
[10] M. Shima, T. Tepper, and C. A. Ross, J. Appl. Phys. **91**, 7920 (2002).
[11] D. Stanoi, G. Socol, C. Grigorescu, F. Guinneton, O. Monnereau, L. Tortet, T. Zhang, and I. N. Milailescu, Mater. Sci. Eng., B **118**, 74 (2005).
[12] N. Umada, H. Yanagihara, A. Hatanaka, and E. Kita, Jpn. J. Appl. Phys., Part 1 **44**, 6538 (2005).
[13] JCPDS Card No. 38-1479.
[14] JCPDS Card No. 32-0285.
[15] JCPDS Card No. 9-0332.
[16] JCPDS Card No. 36-1329.
[17] T. Tsutsumi, I. Ikemoto, T. Namikawa, and H. Kurdo, Bull. Chem. Soc. Jpn. **54**, 913 (1981).
[18] H. Jalili, N. F. Heinig, and K. T. Leung, in *Nanoscale Magnetics and Device Applications*, MRS Symp. Proc. Vol. 998E edited by D. P. Pappas (Materials Research Society, Warrendale, PA, 2007), p. 0998-J05-06.
[19] H. A. Bullen and S. J. Garrett, Surf. Sci. Spectra **8**, 3 (2001); H. A. Bullen and S. J. Garrett, Chem. Mater. **14**, 243 (2002).
[20] B. Liu, Y. Fang, and M. Terano, J. Mol. Catal. A: Chem. **219**, 165 (2004).
[21] R. Cheng, B. Xu, C. N. Borca, A. Scokolov, C. S. Yang, L. Yuan, S. H. Liou, B. Doudin, and P. A. Dowben, Appl. Phys. Lett. **79**, 3122 (2001).
[22] I. Ikemoto, K. Ishii, S. Kinoshita, H. Kuroda, M. A. Alarofranco, and J. M. Thomas, J. Solid State Chem. **17**, 425 (1978).
[23] E. Brand, D. Kellett, M. D. Enever, J. T. Fellows, and R. G. Egdell, J. Mater. Chem. **15**, 1141 (2005).
[24] M. C. Biesinger, C. Brown, J. R. Mycroft, R. D. Davidson, and N. S. McIntyre, Surf. Interface Anal. **36**, 1550 (2004).
[25] D. K. Aswal, K. P. Muthe, S. Tawdw, S. Chohury, N. Bagkar, A. Singh, S. K. Gupta, and J. V. Yakhmi, J. Cryst. Growth **236**, 661 (2002).
[26] D. Shuttleworth, J. Phys. Chem. **84**, 1629 (1980).